Evaluation of a Plasma Impedance Probe in a Time-varying Non-uniform Plasma

Mark A. Hopkins,* and Lyon B. King†
Michigan Technological University, Houghton, MI, 49930

Numerical simulations and experimental measurements were combined to determine the ability of a PIP to measure plasma density and electron collision frequency in a plasma containing spatial gradients as well as time-varying oscillations in the plasma density. Collision frequency was to be measured by the width of the parallel resonance in the real part of plasma impedance-vs.-frequency, while plasma density was to be measured using the zero-crossing of the imaginary impedance-vs.-frequency at parallel resonance. Simulations of the probe characteristic in a plasma gradient indicated that the broadening the real part of plasma impedance due to the spatial gradient obscured the broadening due to electron collision frequency. Simulation results also showed that it may be possible to measure relative changes in electron collision frequencies in a spatial plasma gradient, but the broadening effect of the time-varying oscillations made collision frequency measurements impossible. The time-varying oscillations had the effect of causing multiple zero-crossings in the imaginary part of impedance at parallel resonance. Results of experiments and simulations indicated that the lowest-frequency zero-crossing represented the lowest plasma density in the oscillations and the highest-frequency zero-crossing represented the highest plasma density in the oscillations, thus the PIP probe was found to be an effective tool to measure both the average plasma density as well as the max and min densities due to temporal oscillations.

Nomenclature

C_0	=	vacuum capacitance
C_p	=	plasma capacitance
C_{sh}	=	sheath capacitance
C_{vac}	=	vacuum capacitance of the probe
ε_0	=	permittivity of free space
ε_p	=	relative plasma permittivity
$f_{breathing}$	=	frequency of the breathing mode oscillation

* PhD Candidate, Mechanical Engineering-Engineering Mechanics, 815 R. L. Smith BLDG, AIAA Student Member.

† Ron and Elaine Starr Professor of Space Systems, Mechanical Engineering-Engineering Mechanics, 815 R. L. Smith BLDG, AIAA Member.

f_{noise} = noise in the simulation of electron density oscillations
f_{sample} = sampling frequency of the vector network analyzer
f_{VNA} = output frequency of the vector network analyzer
Δf_{VNA} = frequency step in the vector network analyzer sweep
m_e = electron mass
n_e = electron number density
n_{e0} = amplitude of electron density oscillation
n_{eAve} = average electron number density
n_n = neutral density
ν = electron collision frequency
P = pressure
ρ = radius
σ = collision cross section for xenon
T_e = electron temperature
ω = stimulus frequency
ω_p = plasma frequency
Z = total probe impedance
Z_p = plasma impedance
Z_{sh} = sheath impedance

I. Introduction

DESPITE the ubiquitous use of Langmuir probes as the predominant method of measuring electron temperature and density in laboratory plasmas there are other diagnostic techniques which offer benefits over Langmuir probes for characterizing plasmas. One such diagnostic is the resonance probe. A resonance probe characterizes the plasma not by quantifying the flux of charged particles to a surface, but instead by establishing the interaction between the plasma and a radio-frequency wave emitted from the probe. By intelligently choosing the probe geometry, resonance probes can be impervious to conductive contaminants, dielectric contaminants, and reactive plasmas.

A resonance probe (RP) is an electrically short antenna immersed in a plasma. A radio frequency (RF) signal is applied to the probe and the frequency is swept while antenna characteristics, such as impedance and reflection coefficient, are monitored. Depending on the geometry of the probe, different resonances will be observed whose frequencies are related to electron temperature, plasma density, and electron collision frequency. The physical phenomena which RPs exploit have been known since the 1930s [1]. Research performed in the 1960s demonstrated the feasibility of resonance probes and built a theoretical framework for their use [2-5]. Several different techniques have been developed using resonance probes and have been well characterized [6-13]. One of the simplest techniques was that which was developed by Blackwell et al [11]. Blackwell's technique measures the impedance of a spherical antenna immersed in a plasma using a network analyzer. This technique is desirable due to its simplistic design; it is simply a small conductive sphere (~1 cm in diameter) immersed in a plasma. It can be used in many different plasma environments because it is impervious to dielectric and conductive contaminants [11]. In his experiments, Blackwell determined the plasma density by measuring the plasma frequency through analysis of the imaginary part of the antenna impedance. For this reason his method is known as the plasma impedance method and the probe is known as a plasma impedance probe (PIP).

By definition resonance occurs when the imaginary part of impedance is zero. Series resonance occurs when the impedance of the system is at a minimum (RF short circuit) and parallel resonance occurs when the total impedance

is at a maximum (RF open circuit). It has been shown that for un-magnetized plasmas where electron collision frequency is negligible compared to plasma frequency, parallel resonance occurs at plasma frequency, while series resonance occurs at a slightly lower frequency [3,11]. Because total impedance is at a maximum for parallel resonance, the real part of impedance vs. frequency curve demonstrates a sharp maximum at the plasma frequency. The following derivation will show that the width and height of the peak in the real part of impedance should correlate to the electron collision frequency and that the location of the peak is determined by plasma density.

For the work proposed here, a re-derivation based on the work of Blackwell and Lieberman [11,14] will be performed to disclose the implicit assumptions in the analytic model. The imaginary part of impedance can be used to determine plasma density while the real part of impedance can be used to determine the wave damping coefficient. Since damping occurs as a result of collisions between electrons and other species (either ions, neutrals, or both), a measurement of the damping coefficient can yield a qualitative value for the effective plasma collision frequency. Figure 1 shows a notional experiment that highlights the major components of the plasma impedance method. For the notional experiment we assume a spherical probe is immersed in a low-density plasma. Assuming the probe is not at plasma potential, a sheath will form around the probe. A second sheath will form where the bulk plasma contacts the wall of the vacuum facility.

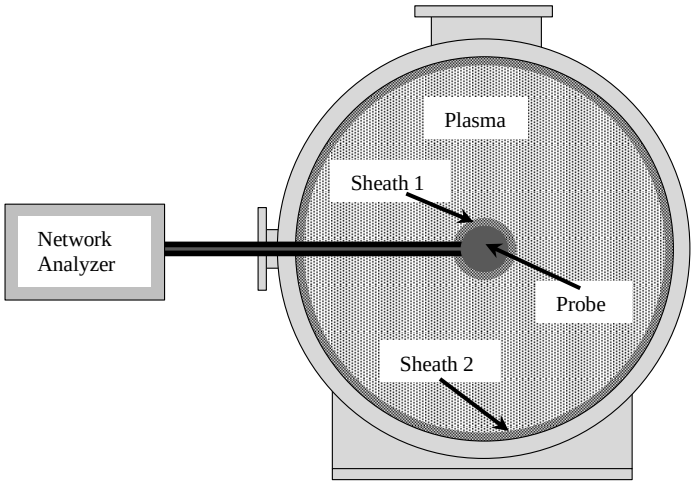

Figure 1. Notional schematic of the plasma impedance method.

First, we start with the total impedance of the probe-plasma system. The total impedance is the sum of the impedance of sheath 1, Z_{sh1}, the bulk plasma, Z_p, and sheath 2, Z_{sh2}, as shown in equation (1).

$$Z = Z_{sh1} + Z_p + Z_{sh2} \tag{1}$$

Because the impedance of the sheath is assumed to be purely capacitive, it takes the form $Z_{sh} = 1/j\omega C_{sh}$, where ω is the driven frequency of the RF, and C_{sh} is the sheath capacitance. Due to the much larger surface area of sheath 2 compared to sheath 1 the impedance of sheath 2 is negligible compared to sheath 1. This leads to the total impedance shown in equation (2).

$$Z = \frac{1}{j\omega C_{sh1}} + Z_p \tag{2}$$

The impedance of the bulk plasma can be determined by approximating the entire system as a large spherical capacitor with a plasma dielectric. Using this construct the impedance of the plasma takes the form:

$$Z_p = \left(j\omega C_p\right)^{-1} = \left(j\omega \frac{4\pi\varepsilon_0\varepsilon_p}{\frac{1}{\rho_1} + \frac{1}{\rho_2}} \right)^{-1} \tag{3}$$

where C_p is the capacitance of the plasma, ε_p is the relative permittivity of the plasma, ρ_1 is the radius of the probe, and ρ_2 is the radius of the vacuum facility. Because $\rho_2 >> \rho_1$ we have:

$$Z_p = \left(j\omega 4\pi\varepsilon_0\varepsilon_p\rho_1 \right)^{-1} \tag{4}$$

Substituting the relative permittivity of an un-magnetized, collisional plasma, $\varepsilon_p = 1 - \frac{\omega_p^2}{\omega(\omega - j\nu)}$ yields:

$$Z_p = \left(j\omega 4\pi\varepsilon_0\rho_1 + \frac{1}{j\omega\left(\omega_p^2 4\pi\varepsilon_0\rho_1\right)^{-1} + \nu\left(\omega_p^2 4\pi\varepsilon_0\rho_1\right)^{-1}} \right)^{-1} \tag{5}$$

where ω_p is the plasma frequency and ν is the total electron collision frequency. By noticing $C_{vac} = 4\pi\varepsilon_0\rho$ is the capacitance of a conducting sphere in an infinite vacuum we can simplify the plasma impedance to its final form in equation (6).

$$Z_p = \left(j\omega C_{vac} + \frac{1}{j\omega\left(\omega_p^2 C_{vac}\right)^{-1} + \nu\left(\omega_p^2 C_{vac}\right)^{-1}} \right)^{-1} \tag{6}$$

Substituting the equation (6) into equation (2) gives the total probe-plasma impedance.

$$Z = \frac{1}{j\omega C_{sh1}} + \frac{1}{j\omega C_{vac} + \frac{1}{j\omega\left(\omega_p^2 C_{vac}\right)^{-1} + \nu\left(\omega_p^2 C_{vac}\right)^{-1}}} \tag{7}$$

Taking the real and imaginary parts of equation (7) yields:

$$\mathrm{Re}[Z] = \frac{\nu\omega_p^2}{C_{vac}\left[\omega^2\nu^2 + \left(\omega^2 - \omega_p^2\right)^2\right]} \tag{8}$$

$$\mathrm{Im}[Z] = \frac{\omega^2 C_{sh}(\omega_p^2 - \omega^2 - \nu^2) - C_0[\omega^2\nu^2 + (\omega^2 - \omega_p^2)^2]}{\omega C_{sh} C_0[\omega^2\nu^2 + (\omega^2 - \omega_p^2)^2]} \tag{9}$$

In equation (8), ν is the damping coefficient and is related to the total electron collision frequency. Since the plasmas examined in this work are low density, low temperature plasmas, the electron-electron and electron-ion collisions are assumed to be negligible compared to the electron-neutral collisions. The neutral density can be extracted from ν using the following equation

$$\nu = \sigma n_n \sqrt{\frac{8T_e}{\pi m_e}} \tag{9}$$

where n_n is the neutral density, T_e is the electron temperature, m_e is the electron mass, and σ is the electron-neutral collision cross-section. Pressure can then be related to n_n through the ideal gas law, $P = nk_BT$.

Plotting equations (8) and (9) for several different facility background pressures—and thus different electron collision frequencies—demonstrates that there should be a discernible change in the impedance characteristic of the probe-plasma system. Figure 2 shows a graph of 10 impedance curves calculated using a background pressure range of 1 x 10^{-5} Torr to 1 x 10^{-4} Torr using xenon gas with a collision cross-section of 16 x 10^{-20} m^2 at T_e = 3 eV [15]. It is clearly visible from the graph that the height and width of the resonance peak in the real impedance curve changes with pressure. For an incremental change in pressure of 1 x 10^{-5} Torr the full width at half maximum (FWHM) of the real impedance is expected to increase ~20 kHz, such that the width of the real impedance curve should be 180 kHz wider at 1 x 10^{-4} Torr than at 1 x 10^{-5} Torr. The curves of Re[Z] vs. frequency reach a maximum at the plasma frequency. Because the plasma frequency can be extracted from the location of the peak as well as from the zero crossing of the Im[Z] vs. frequency, equation (8) could be used to perform a fit on measured real impedance

characteristics from a known antenna geometry where the only free parameter is the collision frequency. It is important to note that changes in plasma density do not affect the height or width of the resonance peak in the real impedance, while changes in electron collision frequency do affect the height and width.

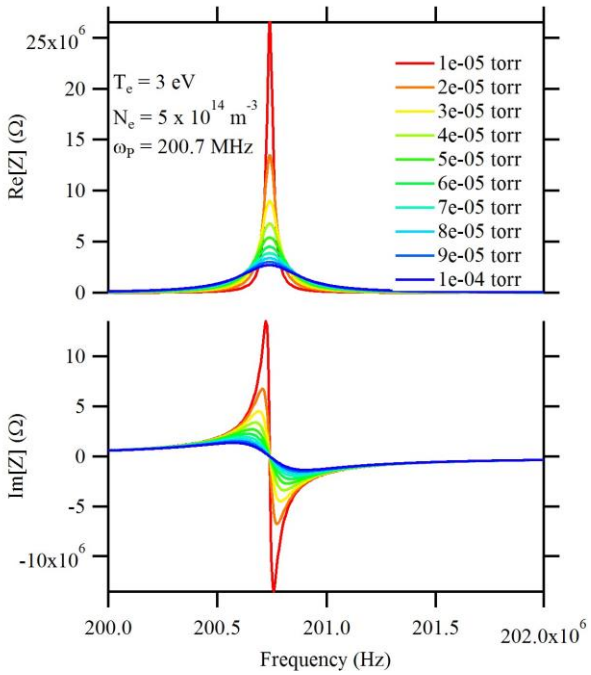

Figure 2. A graph showing several theoretical impedance measurements at xenon pressures ranging from 1 x 10^{-5} Torr to 1 x 10^{-4} Torr for a plasma with an electron number density of 5 x 10^{14} m^{-3} and electron temperature of 3 eV. The maximum of each real curve and the zero-crossing of each imaginary curve occur at plasma frequency. The FWHM of the Re[Z] curve at 1 x 10^{-5} Torr is 22.9 kHz, the FWHM of the 1 x 10^{-4} Torr curve is 192.0 kHz for a total FWHM change of 169.1 kHz over a decade of pressure.

While extensive work has been performed on the use of resonance probes in homogeneous steady plasmas, real laboratory plasmas have spatial gradients in plasma density and, usually, some level of temporal variation. To date no studies have focused on the effects of spatial gradients in electron density, nor on the effect of time varying electron density. Therefore, the goal of the experiments reported here was to evaluate the ability of a plasma impedance probe to measure plasma density and electron collision frequency in a plasma with spatial gradients and time varying density. The results of three studies were combined to fully understand the probe-plasma system: (1) a numerical study of the effect of the plasma gradient on a spherical antenna, (2) a set of experiments in the plasma plume of a Hall-effect thruster for space propulsion, and (3) a numerical study on the effect of plasma density oscillations.

II. Experimental Setup

A Hall-effect thruster was used as a plasma source. Hall thrusters are electric space propulsion devices which used crossed electric and magnetic fields to generate and expel plasma for propulsive purposes. The crossed electric and magnetic fields confine electrons in an azimuthal drift with motion towards the anode limited by cross-field mobility. Gaseous propellant flows through the confined electrons and through electron impact ionization is ionized and accelerated away from the device by the electric field [16-18]. A schematic of a Hall thruster is shown in Figure 3. While Hall thrusters are generally considered to be DC plasma devices, there is an oscillatory component to the discharge known as the thruster breathing mode. The breathing mode is an oscillation in the discharge current of the thruster at approximately 20-30 kHz where the plasma discharge current can oscillate more than ±50% of the

average current measurement [19]. This translates to a commensurate oscillation in the plasma density downstream of the thruster [20].

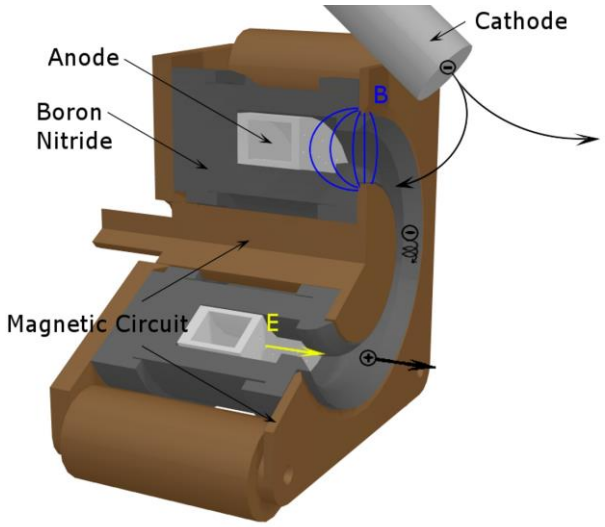

Figure 3. Cross-sectional view of a Hall thruster. Electrons are emitted from the cathode and are drawn to the positive potential of the anode (usually ~300 Volts). The electrons are confined by the radial magnetic field crossed with the axial electric field. Gaseous propellant flows out through pores in the anode and through the confined electrons where it is ionized. Once ionized, the positively charged propellant is accelerated along the axial electric field away from the device.

The thruster used for these experiments was a laboratory Hall thruster modeled after the Aerojet BPT-2000 Hall thruster using a LaB_6 laboratory hollow cathode [21]. Impedance measurements were made with an R&S®ZVL Vector Network Analyzer (VNA) with an output impedance of 50 Ohms. The vacuum facility used for testing was the Xenon Test Facility (XTF) in the Ion Space Propulsion laboratory at Michigan Technological University. The XTF is a 2-m-diameter, by 4-m-long vacuum facility pumped with two cryogenic pumps for a combined pumping speed of 120,000 liters-per-second on nitrogen and a base pressure of 10^{-6} Torr. Pressure was measured with a hot-cathode ionization gauge located at the facility wall. Plasma density in the plume was varied by adjusting the propellant flow to the thruster. A schematic of the experimental setup is shown in Figure 4.

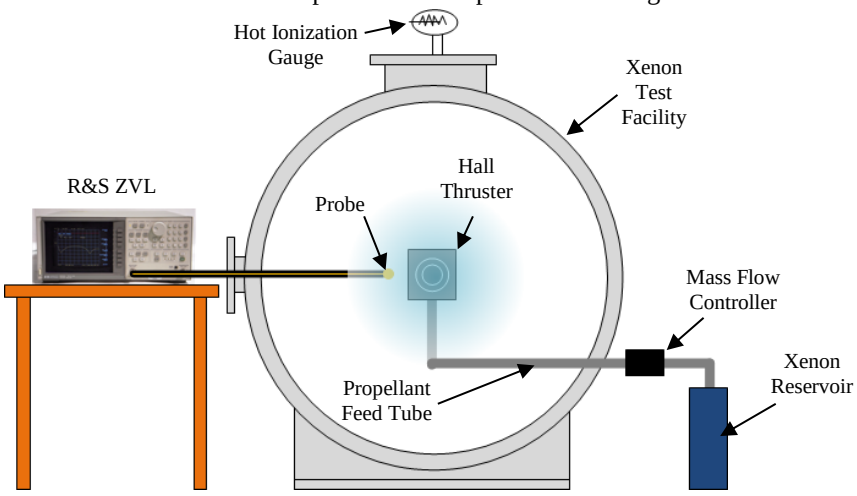

Figure 4. Test schematic. Impedance measurements will be made in the plume of a xenon Hall thruster. Plasma density was varied by changing the propellant flow rate to the thruster.

The plasma impedance probe (PIP) was built to the specifications of Blackwell et al [11] and had a 19-mm-diameter antenna. The spherical antenna was mounted at the end of UT-250C rigid coaxial cable with an SMA connector at the opposite end. The probe was 52 mm from the center of the antenna to the end of the SMA connector. The probe was constructed by first removing the copper shield and insulation from the end of the rigid coax to expose the center conductor. Nine millimeters of the center conductor were exposed and an additional 11 mm of the copper jacket was removed from the coax. Finally the sphere was soldered to the end of the probe. A detailed schematic of the probe is shown below in Figure 5. The probe was connected to the VNA through 91 cm of 50-Ohm UT-250C rigid coaxial cable through an impedance matched 50-Ohm vacuum feedthrough. In order to minimize the effect of the cable a calibration was performed using a calibration kit standard. During calibration, the probe was removed from the assembly and replaced by the calibration kit. A full one-port calibration was performed using an open standard, short standard, and a 50-Ohm, impedance-matched load.

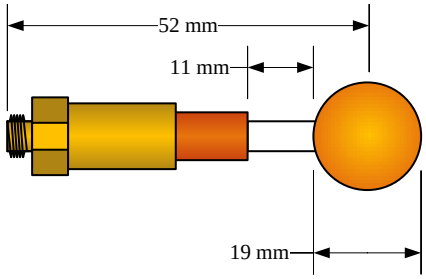

Figure 5. Detailed schematic of the PIP. The probe was constructed by removing the shield and insulation from the rigid coaxial cable to expose 9 mm of the center conductor. The copper jacked was then removed to expose 11 mm of the Teflon insulation. Finally the brass sphere was soldered to the end.

III. Results and Discussion

In order to evaluate the ability of the PIP to measure plasma density and electron collision frequency in a plasma with spatial gradients and time varying density the two effects needed to be isolated. In laboratory plasmas it is impossible to completely eliminate all spatial gradients. Therefor the effects of the spatial gradient were simulated in COMSOL prior to taking measurements in the laboratory.

A. Effect of Spatial Gradient in Density

It was expected that a spatial plasma density gradient would affect the shape of the impedance vs. frequency characteristics. In a non-homogenous plasma the PIP is simultaneously interacting with different regions of plasma density that exist on different sides of the probe. This effect was explored by simulating a spherical antenna immersed in a non-homogenous plasma in COMSOL Multiphysics using an axisymmetric model of a spherical capacitor. The relative permittivity of the capacitor dielectric was set to be that of a collisional plasma:

$$\varepsilon_p = 1 - \frac{\omega_p^2}{\omega(\omega - j\nu)} \tag{10}$$

The Electric Currents module was used for the model and studied in the frequency domain using the stationary solver. The model is described schematically in Figure 6. The radius of the probe was chosen to be 5 mm and the radius of the wall was chosen to be a 1 m, in accordance with the dimensions of the actual probes and the size of the vacuum facility.

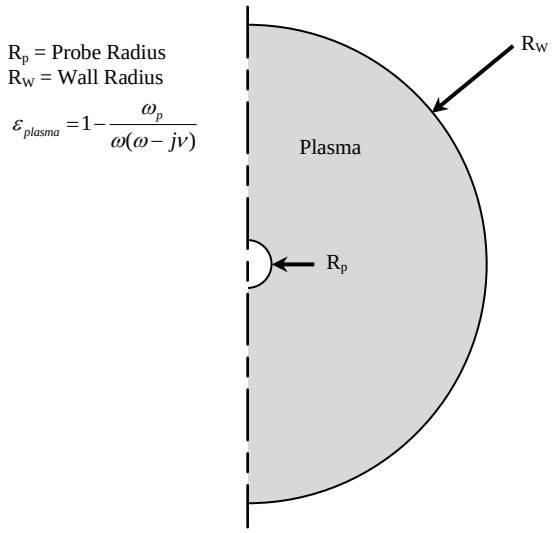

Figure 6. COMSOL model domain.

Before simulating the effect of the plasma gradient, a uniform plasma was simulated and compared to the analytic prediction. The results are shown in Figure 7. For both the simulation and the analytic equation, the plasma density was 5 x 10^{14} m^{-3}, the electron temperature was 3 eV, and the neutral background pressure was 1 x 10^{-4} Torr. The simulation agreed very well with the analytic equation with only a scaling constant—validating the COMSOL calculation. The simulation was then repeated with varying spatial plasma density gradients. A spatially varying plasma density was used as a test field having maximum density of 10 x 10^{-14} m^{-3} and minimum density of 0 m^{-3}; the density was varied linearly with distance while keeping the mid-point density (of 5 x 10^{14} m^{-3}) located at the antenna mid plane. The effect of gradient strength was studied by varying the distance between min and max density within the vacuum chamber envelope. The two distances chosen were 2-m for a weak gradient, and 0.46-m for a strong gradient. The resulting spatial variation in plasma frequency is shown for each simulation in Figure 8. Comparing the real impedance of the antenna in the non-uniform plasma to that simulated in the uniform plasma shows dramatic broadening of two orders-of-magnitude in the FWHM, from 4 kHz to 394 kHz, and a two order-of-magnitude decrease in the peak of the impedance curves. This peak broadening indicates that an absolute measure of electron collision frequency is not possible with a PIP since the broadening effect of the spatial gradient will obscure the slight broadening expected because of electron collisions. While there was a dramatic effect on the shape of the imaginary impedance curve, the location of the zero crossing for parallel impedance occurred at 200.77 MHz correlating to the average density across the surface of the probe of 5 x 10^{14} m^{-3}. These effects on the impedance are highlighted in Figure 9.

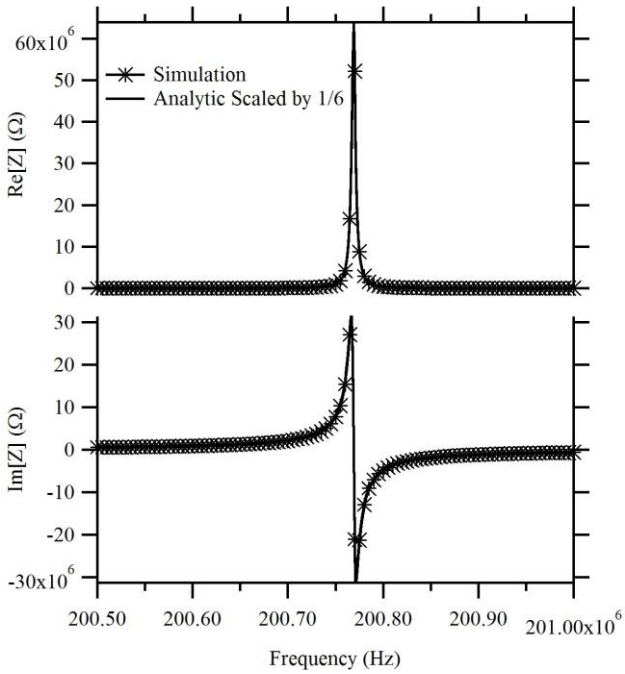

Figure 7. The simulated impedance of a uniform plasma compared to the analytic prediction. For both, the density was 5 x 10^{14} m^{-3}, the electron temperature was 3 eV, and the neutral background pressure was 1 x 10^{-4} torr. The simulation has very good agreement with the analytic equation when the analytic result is scaled down by 1/6.

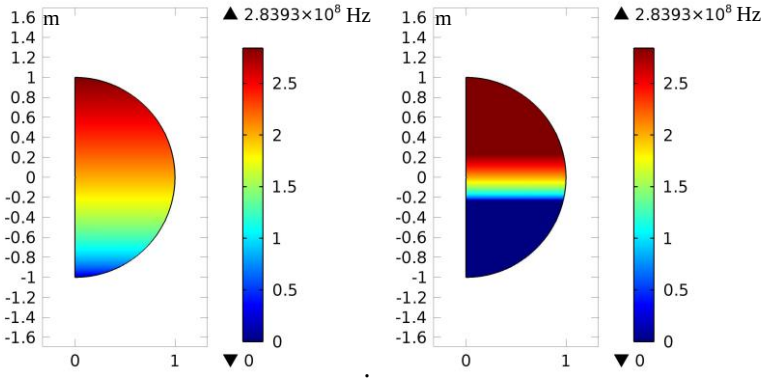

Figure 8. The simulated spatial variation in plasma frequency due to a gradient in plasma density from 10 x 10^{14} m^{-3} to 0 m^{-3} over different distances. LEFT: 2-m gradient. RIGHT: 0.46-m gradient.

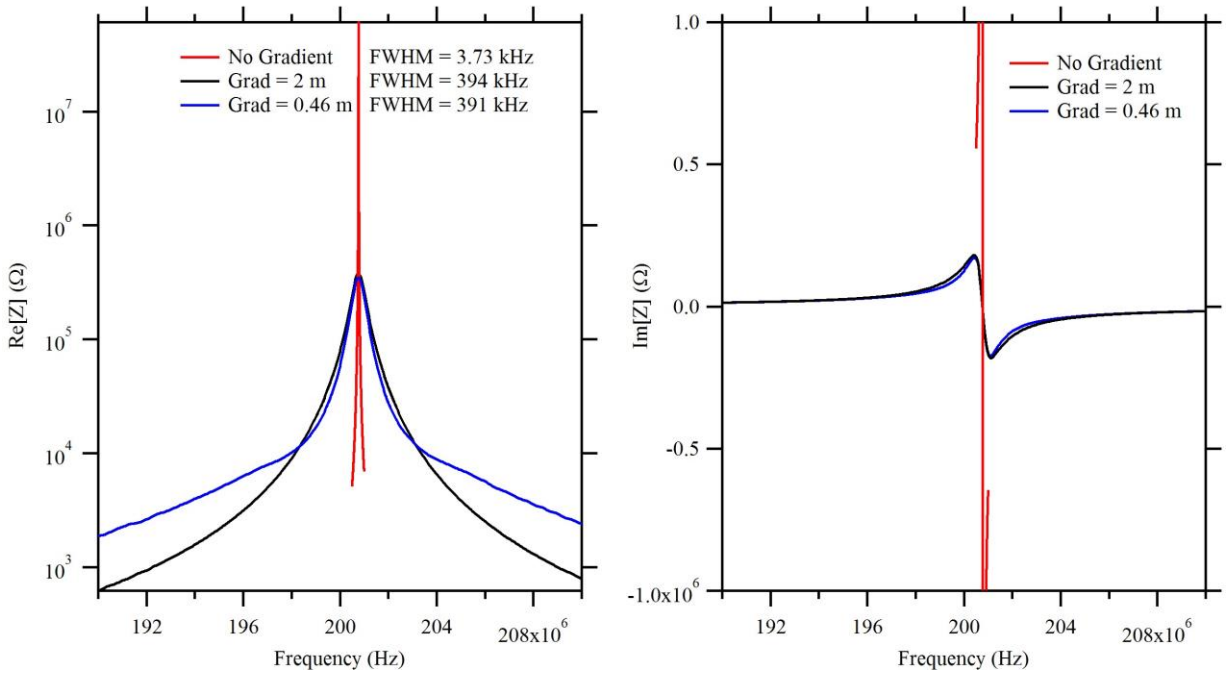

Figure 9. LEFT: The effect of a gradient in plasma density on the real impedance is simulated. There is a two order-of-magnitude difference between the peak of the uniform density simulation verses the peaks of the density gradient simulation and dramatic increase in width from ~4 kHz without gradient to ~400 kHz with the gradient. RIGHT: The effect of a gradient in plasma density on the imaginary impedance. While the shape of the imaginary impedance curves was affected, the zero crossing for parallel resonance was unaffected, preserving the ability to measure an average plasma density in the gradient.

While the broadening caused by the plasma gradient makes measurements of the absolute collision frequency impossible it may still be possible to measure relative changes in collision frequency. For this reason, the last study of the gradient simulation was to test the effect of changing the electron collision frequency while maintaining a constant non-zero plasma gradient. The simulation was run with pressures of 1 x 10^{-4} Torr and 1 x 10^{-5} Torr and the 2-m distance was used to simulate the plasma gradient. The results of the simulation show that the change in collision frequency may still be measured within a plasma gradient. At 1 x 10^{-5} Torr the FWHM was 78.3 kHz, while at 1 x 10^{-4} Torr the FWHM was 394 kHz, just as before, indicating that changes in collision frequency may still be measureable.

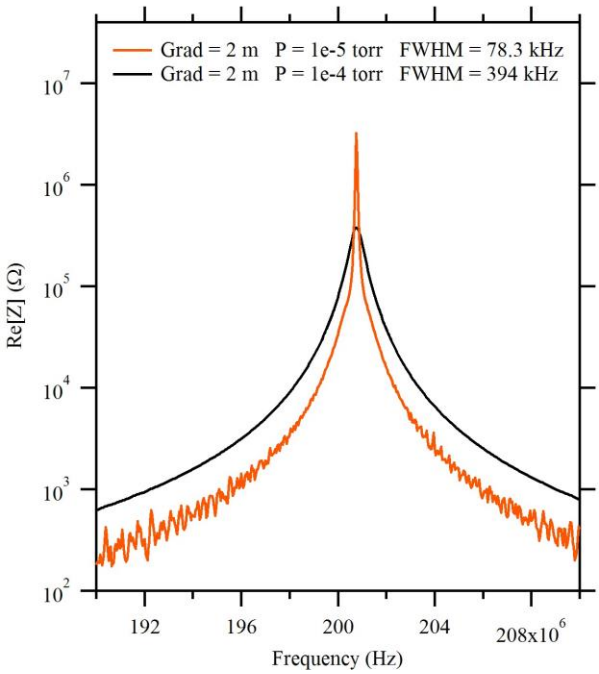

Figure 10. The simulation results showing a change in the background pressure with a plasma gradient. The increase in pressure from 1 x 10^{-5} Torr to 1 x 10^{-4} Torr increased the FWHM from 78 kHz to 394 kHz.

B. Experimental Measurements

The PIP was placed 75-cm downstream of the Hall thruster and 20-cm off of the thrust axis. The thruster was operated with xenon propellant with mass flow rates of 30 SCCM, 50 SCCM, and 70 SCCM such that different plasma densities could be generated. The cathode flow rate was left constant at 5 SCCM. The thruster was operated with a discharge voltage of 300 Volts and the thruster magnet current was tuned at each mass flow rate to minimize discharge current. Minimizing discharge current maximizes the ionization efficiency of the device; the ratio of electrons reaching the anode to ions generated approaches unity. Tuning the magnets also damps the Hall thruster breathing mode oscillation [16,19].

Real and imaginary impedance of the PIP was measured as a function of frequency at each flow rate and the results are shown in Figure 11. As expected, parallel resonance occurred at higher frequencies with increasing thruster mass flow rate indicating a higher plasma density. Plasma density is plotted verses propellant mass flow rate in Figure 12, where the error bars represent the lowest-frequency and highest-frequency zero-crossing (noise width) of the imaginary impedance at parallel resonance. The plasma density ranged from 4 x 10^{14} m^{-3} to 1 x 10^{15} m^{-3} which is in the range expected for the location of the PIP in the thruster plume [22].

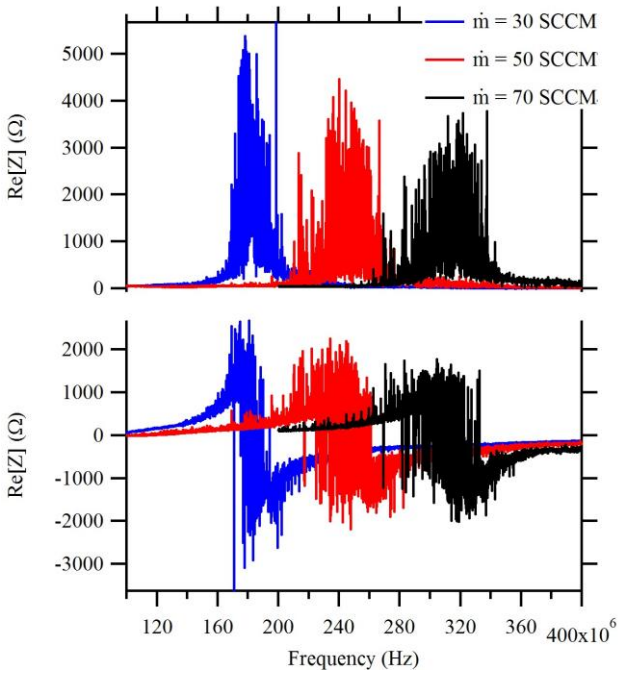

Figure 11. Real and imaginary impedance measurements taken at three different thruster mass flow rates. As expected the parallel resonance in the imaginary impedance occured at increasing frequencies with increasing propellant flow. The width of the resonance in both traces was much larger than expected.

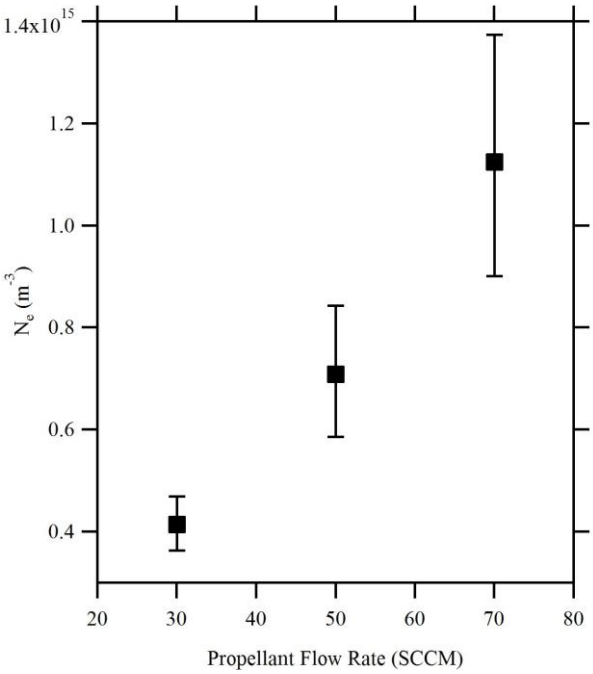

Figure 12. Electron number density verses the thruster mass flow rate. The lower error bar represents the lowest-frequency zero-crossing of the imaginary impedance at parallel resonance and the upper error bar represents the highest-frequency zero-crossing.

While the location of the resonance and corresponding density measurements were within the expected range, the width of the resonance was much larger than expected. For example, the FWHM for the 30 SCCM flow rate was

~21.9 MHz which is two orders-of-magnitude greater than the 400 kHz width predicted in the COMSOL model with the 2-m gradient. The 2-m gradient in plasma density is similar to what is expected in the plume at that location [22] and the result eliminates the possibility of measuring even relative collision frequencies. A hypothesis was formed that the thruster breathing mode may be affecting the impedance measurements. To test the hypothesis an experiment was performed where the thruster magnetic field was intentionally de-tuned from its optimal setting in order to induce high amplitude current oscillations while taking measurements with the PIP. The intent was to induce temporal density oscillations in the plasma without greatly affecting the average plasma density. In order to induce larger oscillations in the discharge current, the magnet current was incrementally decreased from 2.00 Amps to 1.25 Amps by 0.25 Amp increments. At each magnet current, the discharge current was measured on an oscilloscope while simultaneously recording impedance-vs.-frequency traces on the PIP. Figure 13 shows the effect of increasing the magnitude of current oscillations.

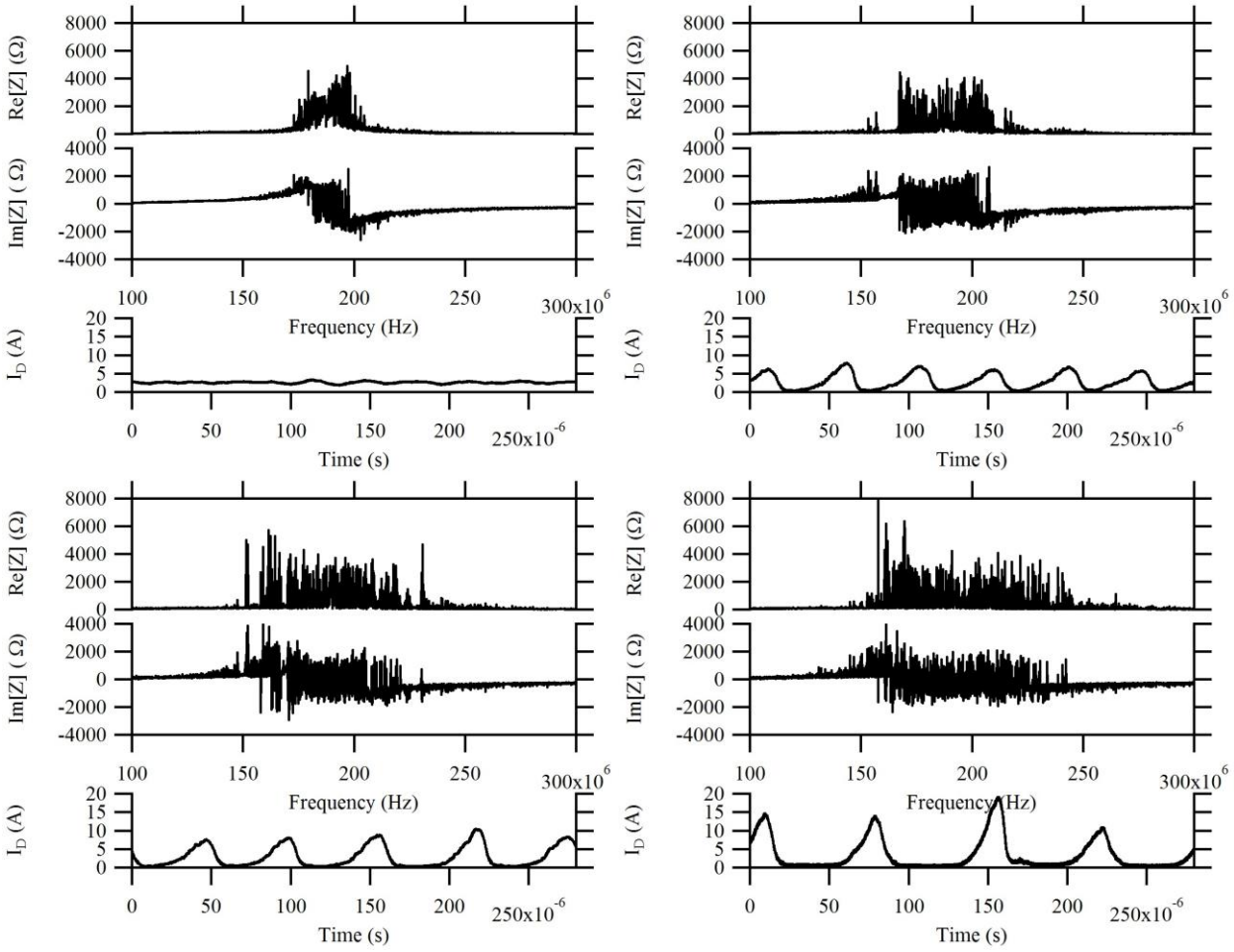

Figure 13. Plots of the real and imaginary PIP impedance along with measurements of the thruster discharge current oscillations. The thruster magnet current was, from the upper left clockwise, 2.00 Amps, 1.75 Amps, 1.50 Amps, and 1.25 Amps. The width of the resonance clearly increases with increasing magnitude of the discharge current oscillations.

As expected, the magnitude of the discharge current oscillations increased with the decrease in the magnet current. For the 2.00-Amp case the discharge current oscillations had a peak-to-peak amplitude of 1.62 Amps at 31 kHz; for the 1.75-Amp case the oscillations had a peak-to-peak amplitude of 7.69 Amps at 22 kHz; the 1.50-Amp case had a peak-to-peak amplitude of 10.3 Amps at 18 kHz; and the 1.25-Amp case had a peak-to-peak amplitude of 19.1 Amps at 13 kHz. The effect of increased magnitude of the breathing mode oscillation is seen in the impedance

measurements as a drastic broadening in the curves, as well as a large increase in the measurement noise. The width of the real impedance curve increases from 24 MHz to 85 MHz when changing the thruster magnet current from 2.00-Amp case (upper left) to the 1.25-Amp magnet case (lower right). A similar broadening occurred in the imaginary impedance. The width of the zero crossing of the imaginary impedance is 14.5 MHz in the 2 Amp case, and 61 MHz wide in the 1.25 Amp case. Figure 14 shows a plot of PIP-derived plasma density as a function of the peak-to-peak amplitude of the discharge current oscillations with the error bars correlating to the lowest- and highest-frequency zero-crossings of the imaginary impedance.

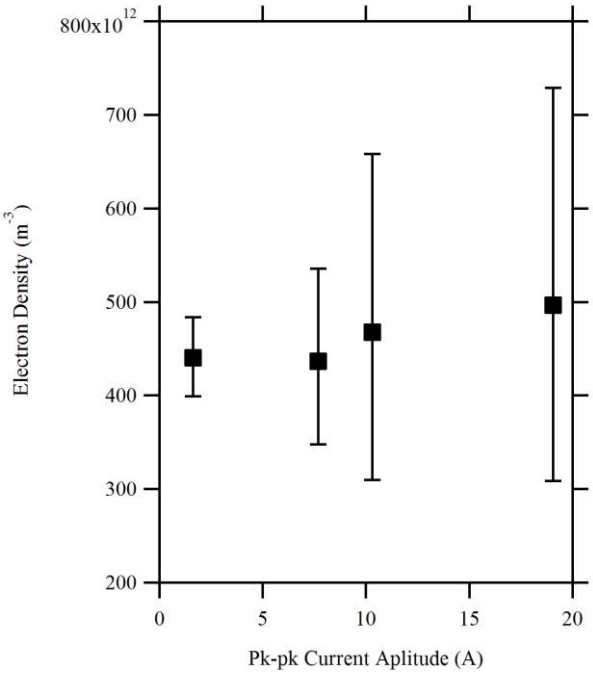

Figure 14. PIP density measurements as a function of peak-to-peak discharge current oscillations. As oscillation amplitude increases so too does the error in the density measurement.

C. COMSOL Simulation of Breathing Mode Oscillations

The broadening of the impedance measurements due to the oscillation of the discharge current is not surprising when one considers the timing involved in measuring the PIP impedance trace. With the test equipment used in this experiment a 4001-point VNA acquisition wherein the impedance is measured over the frequency range from 10 Hz to 400 MHz takes approximately one second to complete. In this same time period thousands of oscillations in the plasma density occur. As a result, the PIP is immersed in different plasma conditions at each measurement step within the frequency trace.

Given the known VNA sampling frequency and plasma oscillation frequency it is possible to simulate the resulting measurements using COMSOL by creating a synthetic time-varying plasma density. To visualize the aliasing the plasma density was modeled as a sinusoid of the following form:

$$n_e(t) = n_{e0}\cos(2\pi f_{breathing} t) + n_{eAve} \tag{11}$$

such that the plasma density oscillated about n_{eAve} at the breathing mode frequency with an amplitude of n_{e0}. Since the simulation operates in the frequency domain, the time component in equation (11) must be written as a function of the VNA output frequency, f_{VNA}. In the time domain the output frequency of the VNA can be written as

$$f_{VNA} = \frac{\Delta f_{VNA}}{1/f_{sample}} t \tag{11}$$

where Δf_{VNA} is the VNA frequency step, and f_{sample} is the sampling frequency of the VNA. Solving for t in equation (11) and substituting it into equation (11) gives an equation for electron density as a function of VNA frequency.

$$n_e(f_{VNA}) = n_{e0}\cos\left(2\pi\frac{f_{breathing}\,f_{VNA}}{\Delta f_{VNA}\,f_{sample}}\right) + n_{eAve} \tag{11}$$

Finally, because the frequency of the thruster breathing mode is not constant a uniform noise term was added to the denominator of equation (11), yielding:

$$n_e(f_{VNA}) = n_{e0}\cos\left(2\pi\frac{f_{breathing}\,f_{VNA}}{\Delta f_{VNA}\left(f_{sample}+f_{noise}\right)}\right) + n_{eAve} \tag{11}$$

Because the plasma permittivity depends on the plasma density, equation (11) leads to a "synthetic" plasma permittivity which depends on the frequency of the VNA, $\varepsilon_p = \varepsilon_p(f_{VNA})$, reflecting the fact that each VNA measurement occurs in a "different" plasma.

For the simulation, n_{e0} = 2.5 x 10^{14} m^{-3}, n_{eAve} = 10 x 10^{14} m^{-3}, $f_{breathing}$ = 25 kHz, f_{sample} = 4000 kHz, f_{noise} = ±500 Hz (uniformly distributed), with a plasma gradient distance of 2 m such that n_{eAve} = 5 x 10^{14} m^{-3} on the centerline of the antenna with a variance of ±1.25 x 10^{14} m^{-3}. The electron temperature and background pressure were 3 eV and 1 x 10^{-4} Torr. The results of the simulation are shown in Figure 15. In the graph, the effect of the breathing mode simulation is shown in black with a comparison to the gradient broadening from the 2-m gradient simulation from Section A in blue. It can be seen from the simulation that there is a significant amount of broadening due to the aliasing from the sample rate of the VNA. The gradient broadened curve has a FWHM of 393 kHz compared to a width of 48 MHz for the aliased curve. The nature of the broadening indicates that the width of the parallel resonance correlates to the minimum and maximum densities of the plasma oscillation. The lowest-frequency zero-crossing of the imaginary impedance correlates to an electron density of 3.8 x 10^{14} m^{-3}, while the highest frequency zero-crossing of the imaginary impedance correlates to an electron density of 6.2 x 10^{14} m^{-3}.

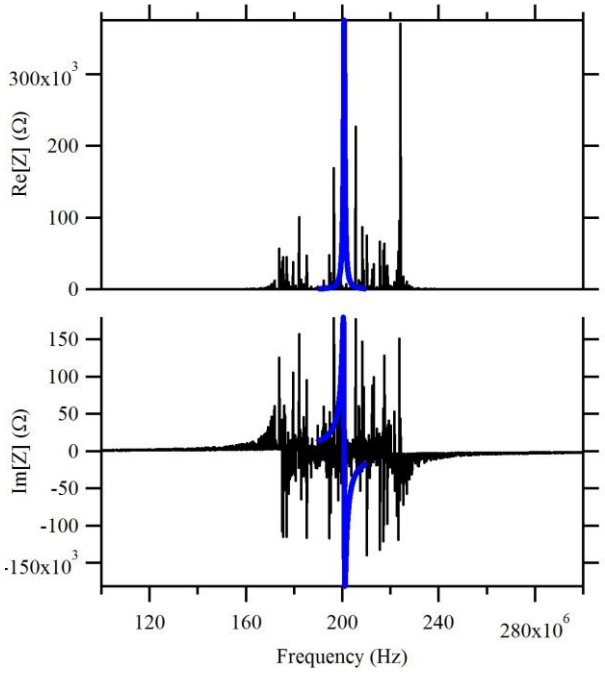

Figure 15. The effect of the VNA aliasing is shown in solid black. The solid gray curve is a gradient broadened curve with the same nominal plasma density.

The results of the simulation indicate that the width of the parallel resonance in the imaginary part of impedance correlates to the minimum and maximum densities of the plasma oscillations. Applying this theory to the data collected in section B, implies that the error bars in Figure 12 and Figure 14 give a true indication of the variance in plasma density.

IV. Conclusions/Future Work

The goal of this paper was to evaluate the ability of the plasma impedance probe to measure the electron density and electron collision frequency in a plasma with a spatial gradient in density as well as a time-varying electron density. It was concluded that the PIP is not a good approach for measuring the absolute plasma collision frequency in a spatially varying laboratory plasma because of the broadening caused by the density gradient. Relative measures of collision frequency may be possible, but the temporal density oscillations present in the plasma used for this study made even relative measurement of collision frequency impossible. Because the plasma under study here varied in density by ±10-20% with a frequency of ~ 20kHz the resulting impedance-vs.-frequency traces showed an effective width of 22 MHz—a width that obscured any relative broadening that could be attributed to changes in neutral pressure. The broadening due to temporal oscillations could perhaps be avoided in future experiments if an impedance curve was recorded by triggering off of the discharge current in some manner to ensure each point within the impedance-vs.-frequency curve was recorded at the same phase of the discharge current oscillation.

The results of this investigation show that the PIP technique yields a good measurement of average electron density even with strong spatial gradients. In the presence of an oscillatory plasma the parallel resonance in the imaginary impedance gives an estimate in the range of plasma densities encountered during a sweep. Experimental data showed variations in density from ±13% for the 30 SCCM experiment to ±20% for the 70 SCCM experiment, with tuned magnetic current. If the measurements of PIP impedance were regularly triggered from the plasma oscillations in a phase-consistent manner the uncertainty in measured plasma density could be greatly reduced. Using the phase-consistent triggering, measures of density-vs.-oscillation phase could be produced giving a visualization of the time-varying oscillations.

Acknowledgments

The authors would like to thank the members of the Ion Space Propulsion lab, Kurt Terhune and Edmond (EJ) Meyer. Particular thanks are due to EJ for offering solutions to many of the problems with the RF antenna. Additional thanks go to Dr. Warren Perger for lending the network analyzer to the project and for helping to interpret the initial data. The authors would also like to thank Dr. Sven Bilén for lending a calibration kit for the project as well as for helping to interpret experimental data. This material is based upon work supported by the National Science Foundation Graduate Research Fellowship Program under Grant No. DGE-1051031. Any opinion, findings, and conclusions or recommendations expressed in this material are those of the authors and do not necessarily reflect the views of the National Science Foundation.

References

[1] Tonks, L., "The High Frequency Behavior of a Plasma," Physical Review Letters, 37, 1931, pp. 1458-1483
[2] Harp, R.S., "The Behavior of the Resonance Probe in a Plasma," Applied Physics Letters, 4, 1964, pp. 186-188
[3] Harp, R.S. and F.W. Crawford, "Characteristics of the Plasma Resonance Probe," Journal of Applied Physics, 35, 1964, pp. 3436-3446
[4] Takayama, K., H. Ikegami, and S. Miyazaki, "Plasma Resonance in a Radio-Frequency Probe," Physical Review Letters, 5, 1960, pp. 238-240
[5] Dote, T. and T. Ichimiya, "Characteristics of Resonance Probes," Journal of Applied Physics, 36, 1965, pp. 1866-1872
[6] Stenzel, R.L., "Microwave resonator probe for localized density measurements in weakly magnetized plasmas," Review of Scientific Instruments, 47, 1976, pp. 603-607
[7] Piejak, R.B., et al., "The hairpin resonator: A plasma density measuring technique revisted," Journal of Applied Physics, 95, 2004, pp. 3785-3791

[8] Bilen, S.G., et al., "Resonance-Probe Measurements of Plasma Densities in Electric-Propulsion Plumes," *35th AIAA/ASME/SAE/ASEE Joint Propulsion Conference and Exhibit*, AIAA 99-2714, Los Angeles, California, 20-24 June 1999

[9] Kokura, H., et al., "Plasma Absorption Probe for Measuring Electron Density in an Envirenement Soild with Processing Plasmas," Japanes Journal of Applied Physics, 38, 1999, pp. 5262-5266

[10] Shirakawa, T., "Plasma Oscillation Method for Measurements of Absolute Electron Density in Plasma," Japanes Journal of Applied Physics, 32, 11A, 1993, pp. 5129-5135

[11] Blackwell, D.D., D.N. Walker, and W.E. Amatucci, "Measurement of absolute electron density with a plasma impedance probe," Review of Scientific Instruments, 76, 2005, pp.

[12] Lapke, M., T. Mussenbrock, and R.P. Brinkmann, "The multipole resonance probe: A concept for simultaneous determination of plasma density, electrontemperature, and collision rate in low-pressure plasmas," Applied Physics Letters, 93, 051502 (2008); 10.1063/1.2966351

[13] Lapke, M., et al., "The multipole resonance probe: characterization of a prototype," Plasma Sources Science and Technology, 20, 042001 (2011); 10.1088/0963-0252/20/4/042001

[14] Lieberman, M.A. and A.J. Lichtenberg, *Principles of Plasma Discharges and Materials Processing*2005, Hoboken, NJ: John Wiley & Sons, Inc.

[15] Hayashi, M., "Determination of electron-xenon total excitation cross-sections, from threshold to 100 eV, from experimental values of Townsend's," Journal of Physics D: Applied Physics, 16, 1982, pp. 581-589

[16] Kim, V., "Main Physical Features and Processes Determining the Performance of Stationary Plasma Thrusters," Journal of Propulsion and Power, 14, 1998, pp. 736-743

[17] Hofer, R.R., "Development and Characterization of High-Efficiency, High-Specific Impulse Xenon Hall Thrusters," *Doctoral Dissertaion*, Aerospace Engineering, University of Michigan, 2004

[18] Goebel, D.M. and I. Katz, *Fundamentals of electric propulsion: ion and Hall thrusters*. Vol. 1. 2008: Wiley.

[19] Choueiri, E.Y., "Plasma oscillations in Hall thrusters," Physics of Plasmas, 8, 2001, pp. 1411-1426

[20] Lobbia, R.B., "A Time-resolved Investigation of the Hall Thruster Breathing Mode," *Doctoral Dissertation*, Aerospace Engineering, University of Michigan, 2010

[21] King, D., et al., "Development of the BPT Family of US-Designed Hall Current Thrusters for Commercial LEO and GEO Applications," *34th AIAA./ASME/SAE/ASEE Joint Propulsion Conference & Exhibit*, AIAA-1998-3338, Cleveland, OH,

[22] Boyd, I. and R.A. Dressler, "Far field modeling of the plasma plume of a Hall thruster," Journal of Applied Physics, 92, 2002, pp. 1764-1774